STRESS ANALYSIS OF DIE CASTINGS TAKING INTO ACCOUNT DATA FROM COMPUTED TOMOGRAPHY

Ulrich Gabbert[1], Stefan Ringwelski[2], Mathias Würkner[3], Mario Kittsteiner[4]

1-3 Otto von Guericke University Magdeburg, Germany, ulrich.gabbert@ovgu.de
4- Schaeffler Technologies AG & Co. KG, Germany, mario.kittsteiner@schaeffler.com

Abstract

Pores and shrink holes are unavoidable defects in the die-casting mass production which influence the strength, fatigue and fracture behaviour and, consequently, reduce the life span of a structure. Defects can be detected with computed tomography (CT) measurements and should be considered during the design process or after production, which is usually not done in today's mass production. The paper proposes an effective methodology for the stress analysis of die-cast parts with pores found from CT measurements or that are artificially placed within a structure. The method consists of a combination of the finite element method (FEM) and the finite cell method (FCM), which extends the FEM if the geometry cuts finite elements. This procedure has the advantage that all simulations with different pore distributions, real or artificial one, can be calculated without changing the base finite element mesh. The STL data of defects received from CT measurements cannot be used without repairing them. Therefore, an appropriate repair procedure is proposed first. The coupling procedure of the FEM with the FCM is presented and it is successfully realized in the frame of the commercial software tool Abaqus. The developed software has been successfully tested on academic examples as well as a complex industrial project presented in the paper. The proposed approach could become a preferred way to consider pores in practical applications, where the porosity can be derived either from CT measurements or are artificially adopted for design purposes.

Keywords: *Die-cast parts with pores, stress analysis, computed tomography (CT), repair of STL data, finite element method (FEM), finite cell method (FCM).*

1. Introduction

The application of die-casting technology is an efficient process in the mass production of aluminium and magnesium parts in many fields, such as in the automotive and aerospace industries, electrical engineering, wind power industries, machine and plant engineering, and container construction among many others [1]. One of the basic problems of the die-casting process is the unavoidable porosity of the produced parts [2]. Figure 1 shows a computed tomography (CT) image of an aluminum die-cast housing of a gear box with large pores. Casted parts with surface pores are usually rejected. Most pores exist within the body and are not exposed to the outside unless they are later penetrated during post-machining. The existence of such pores is normally not apparent unless the part is subjected to a computed tomography (CT) scan after casting [3]. A CT

measurement results in a data set containing the three-dimensional coordinates of each voxel (pixel) as well as the Hounsfield value related to a radiodensity scale. The Hounsfield scale is a measure of the weakening of the X-rays and results in a grayscale image. The Hounsfield value of a pixel can be used for the distinction between different materials such as aluminium and air in an aluminium die-cast part with pores (see Figure 1). Based

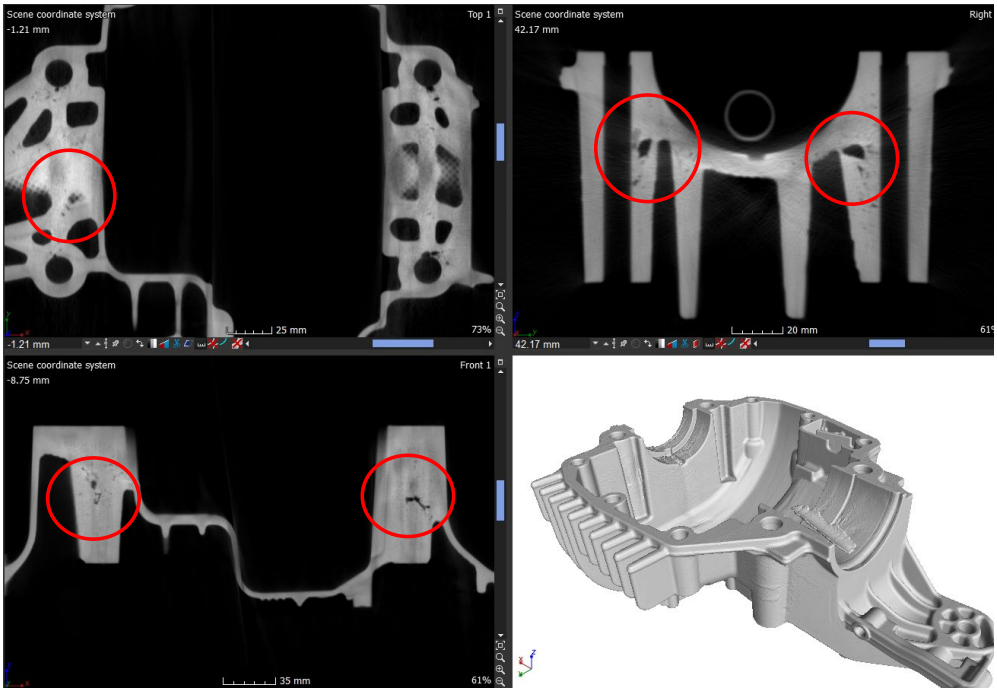

Figure 1. Large pores marked in red in a gear housing found with CT measurements

on the Hounsfield scale different geometrical objects can be identified from CT measurements and described in the form of an STL data set (STL: Standard Tessellation Language). The STL format is supported by many software packages and widely applied in computer aided manufacturing and rapid prototyping. STL files describe the surface geometry of a three-dimensional object, such as a pore, with a triangular surface mesh and can be directly introduced into the FEM meshing procedure [4], [5]. The Hounsfield scale is a measure of the weakening of the X-rays and results in a grayscale image. The Hounsfield value of a pixel can be used for the distinction between different materials such as aluminium and air in an aluminium die-cast part with pores (see Figure 1). Based on the Hounsfield scale different geometrical objects can be identified from CT measurements and described in the form of an STL data set (STL: Standard Tessellation Language). The STL format is supported by many software packages and widely applied in computer aided manufacturing and rapid prototyping. STL files describe the surface geometry of a three-dimensional object, such as a pore, with a triangular surface mesh and can be directly introduced into the FEM meshing procedure [4], [5]. The STL surface data automatically generated from CT measurements should describe a closed and unique surface topology. But this is, unfortunately, most often not the case and has resulted in a lot of

research activities and software developments to repair the STL data [6], [7]. The most promising approach to avoid finite element meshes, which fit with the geometry of the structure under consideration, is the application of the finite cell method (FCM) [8], [9]. The finite cell method has great advantages for structures if the porosity only occurs in small regions as it is often the case in die-cast parts. The remaining parts can be approximated efficiently by the classical FEM method such resulting in a mixed FEM-FCM approach. For industrial applications it would be of a great advantage if the FCM could be incorporated into a commercial FEM software tool. Such a combination of the FEM and the FCM is first time proposed in [10]. In the vicinity of pores, notch stresses are expected, which have to be analysed to answer such questions as: (i) are the notch stresses larger than the allowable stress level, (ii) can the notch stresses cause an unstable crack growth, (iii) do the notch stresses contribute to a reduction of the life span of the construction?

The paper is organized as follows. In Section 2 the STL data from computed tomography are analysed and methods for repairing the data are proposed. In Section 3 the fundamentals of the FCM are briefly discussed and the concept of an overall workflow to combine the FCM with the commercial FEM software tool *Abaqus* is presented and tested. The advantage of such an approach is that any number of pore distributions can be analysed in parallel based on a single finite element basis mesh. In Section 4 an industrial application is presented and the proposed method is applied and compared with the results received with a pure FEM analysis. Section 5 concludes this paper with a summary and an outlook to future developments.

2. The Repair of STL Data

The voxel data of a CT measurement can be processed to obtain a boundary representation via a surface triangulation by using the surface tessellation language (STL) [4], [5], [11]. For simulation reasons it is required that the STL surface mesh describes a closed and unique boundary. But this usually not the case. The obtained STL data very often describing unclosed surfaces, overlapping facets, and incorrect normal directions. Additionally, two closed surface triangulations are sometimes connected to each other, as for instance by a line segment or by a point (Figure 2).

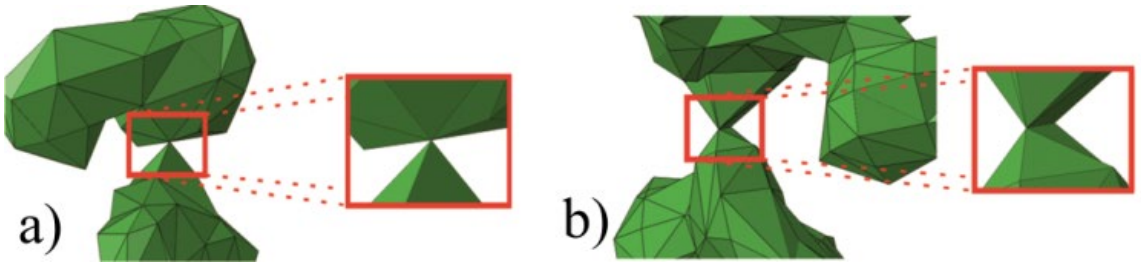

Figure 2. a) Two surfaces connected by a point. b) Two surfaces connected by a line.

The above-mentioned problems complicate a unique identification of surface regions in

an automated algorithm. Therefore, a mesh repair or a remeshing procedure is absolutely essential [12], [13]. There are several software tools available for mesh repairing, which have been mainly developed for 3D printing in medicine. But, if the STL data set is to be used for FEM simulations additional mesh criteria become important as well. FEM stress and strain analysis requires meshes fulfilling the convergence criteria of the FEM, such as avoiding singularities by sharp corners and severely distorted elements. An optimized FEM surface mesh should also have an uniform distribution of triangles of roughly the same size and it should be possible to automatically extend and reduce the number of surface triangles. From a computational point of view, acute triangles should be avoided as well, where two connecting edges of two triangles sharing the same nodal point or two connecting surfaces sharing the same edge should not include very small angles. After testing several software tools, the decision was made in favor of the *Geometry Preparation* tool of the *Simcenter* software (Anderl 2018), which is possible to repair a STL file and transform it into a mesh acceptable for FEM simulations. Figure 3a shows a original STL model of a pore received from the CT measurement device and Figure 3b shows the STL data after repair with help of the *Simcenter* software.

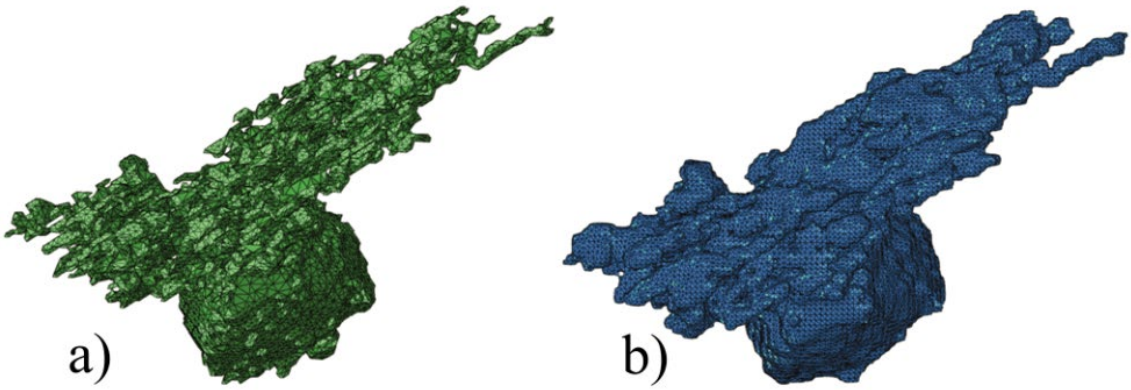

Figure 3. a) Original STL visualization of a pore. b) Repaired pore with the help of *Simcenter*

The repaired STL data are independent from the basis geometry of the pores as well as the mesh density of the triangulated surface mesh. The mesh generation is based on algorithms that generate a new mesh from an original old one in the form of a tight shell surface. It is obvious that the new generated surface is tighter to the original geometry the finer the surface mesh is. The coarser the mesh is, the more geometrical details of a pore are lost. This is accompanied by an increase in the volume of the pore. From a simulation point of view this is normally not a problem, as the structure is weakened mechanically more significantly if the pores in the simulation are larger than in reality [14].

3. A Coupled FEM-FCM Approach

3.1 Brief description of the FCM

The FCM only slightly differs from the FEM. In order to solve a problem with the help of the FEM, a mesh of finite elements is required, which approximately coincide with the geometry of the structural region of interest Ω. However, in the FCM the mesh is not required to fit the structural geometry. The physical domain Ω is extended by a fictitious domain Ω_{fic}. The union of these two domains forms the extended domain Ω_{ex}, see Figure 4.

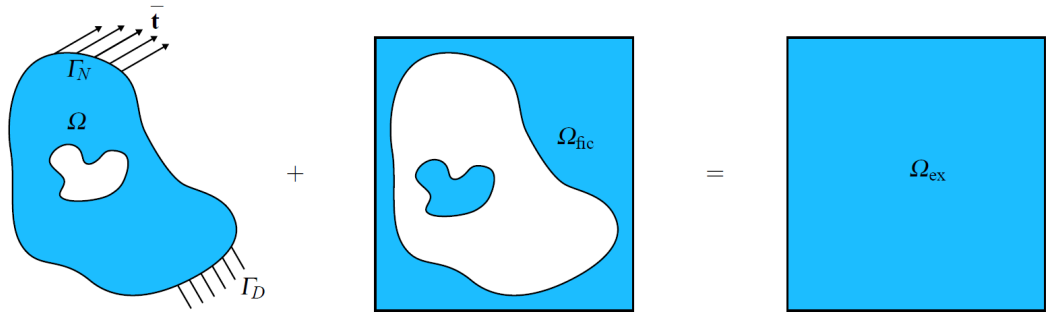

(a) Physical domain Ω (b) Fictitious domain Ω_{fic} (c) Extended domain Ω_{ex}

Figure 4. The fictitious domain approach

The weak form is now solved over the extended region

$$B_{ex}(\boldsymbol{u},\boldsymbol{v}) = F_{ex}(\boldsymbol{v}), \qquad \forall \boldsymbol{v} \in V. \tag{1}$$

Here $\boldsymbol{u}$ is the displacement vector and $\boldsymbol{v}$ represent the vector of arbitrary test functions in the space V of admissible functions. The main advantage of the fictitious domain approach is that the extended domain is of a much simpler geometry and can, therefore, be simply meshed by regular non-distorted finite elements. Quadrilateral and hexagonal elements and triangular and tetrahedral elements can be used for 2D and 3D problems, respectively. During the analysis it is important to distinguish between normal finite elements and those elements that are cut by the physical boundary. This differentiation is controlled by the so-called indicator function α as

$$\alpha(\boldsymbol{x}) = \begin{cases} 1 & \forall \boldsymbol{x} \in \Omega \\ a_0 = 10^{-q} & \forall \boldsymbol{x} \in \Omega_{ex} \backslash \Omega \end{cases}. \tag{2}$$

If $\boldsymbol{x}$ lies in the fictitious region, the indicator function can be taken as zero. However, in order to avoid numerical problems a small value α_0 is typically used instead of zero. The exponent q is typically taken in the range from 4 to 15, depending on the material properties (Duczek, 2014). With the value α, the bilinear form B and the linear form F are given as follows

$$B_{ex}(\boldsymbol{u},\boldsymbol{v}) = \int_{\Omega_{ex}} [\boldsymbol{L}\boldsymbol{v}]^T \, \alpha \boldsymbol{C} [\boldsymbol{L}\boldsymbol{u}] d\Omega, \tag{3}$$

$$F_{ex}(\boldsymbol{v}) = \int_{\Omega_{ex}} \boldsymbol{v}^T \alpha \bar{\boldsymbol{f}} d\Omega + \int_{\Gamma_N} \boldsymbol{v}^T \bar{\boldsymbol{t}} d\Gamma. \tag{4}$$

Here $\boldsymbol{L}$ denotes the linear strain-displacement operator, $\boldsymbol{C}$ stands for Hooke's elasticity matrix, $\boldsymbol{f}$ denotes the vector of body forces and $\boldsymbol{t}$ is the traction vector. A bar over a variable signifies a prescribed value. The prescribed tractions are defined on the Neumann boundary Γ_N

$$\boldsymbol{\sigma}\boldsymbol{n} = \bar{\boldsymbol{t}} \quad \text{on } \Gamma_N, \tag{5}$$

where here $\boldsymbol{\sigma}$ denotes the stress tensor and $\boldsymbol{n}$ constitutes the outward normal vector of unit length. Furthermore, the displacements are prescribed on the Dirichlet boundary Γ_D as

$$\boldsymbol{u} = \bar{\boldsymbol{u}} \quad \text{on } \Gamma_D. \tag{6}$$

The indicator function α allows the distinction between points that are located in Ω or in Ω_{fic}. The problem now arises that the numerical integration of the element matrices of the cut elements has to be performed over discontinuous integrands. The usual applied Gaussian integration of the element matrices is in such cases not accurate enough. Therefore, an adaptive Gaussian integration rule is recommended [8], which can be applied automatically in 2D as well as in 3D finite elements without any extra manual input. For this purpose, a space tree partitioning (e.g. a quadtree in 2D and an octree in 3D) of the integration domain is executed, and in each cut element of the extended region Ω_{ex} a Gaussian integration rule is used. The partitioning is carried out as long as the solution of the integral is approximated sufficiently accurately (see Figure 6). Alternatively, to the space tree subdivision an efficient integration scheme based on the divergence theorem, the Gauß–Ostrogradsky theorem, can be applied which reduces the dimension of the integrals by one. This means that instead of solving the integral for the whole domain only its contour needs to be considered [16].

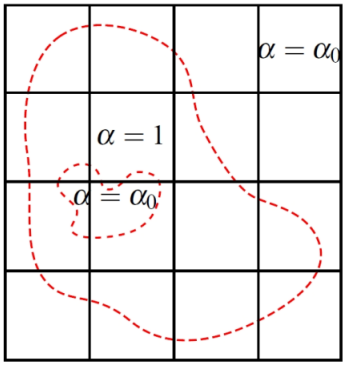

Figure 5. Finite cell discretization

Following the standard Bubnov-Galerkin procedure, the displacement field as well as the test function in each finite element e is approximated as

$$\boldsymbol{u}_e = \mathbf{N}_e \mathbf{U}_e, \tag{7}$$

$$\boldsymbol{v}_e = \mathbf{N}_e \mathbf{V}_e. \tag{8}$$

Here $\mathbf{N}_e$ contains the element shape functions, $\mathbf{U}_e$ represents the vector of unknowns, and $\mathbf{V}_e$ stands for the coefficients of the test functions for one single finite element, which in the context of the FCM is usually named a finite cell. Inserting the Equations (7) and (8)

into the weak form finally yields the well-known linear system of equations

$$\mathbf{KU} = \mathbf{F}, \tag{9}$$

where **K** denotes the global stiffness matrix and **F** represents the global load vector.

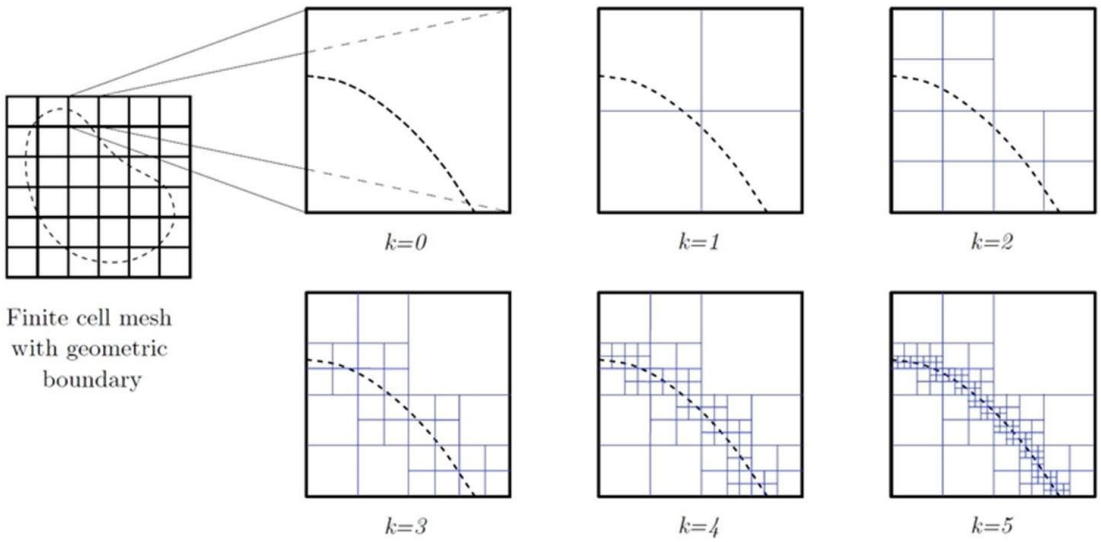

Figure 6. Adaptive subdivision of one element in integration cells

The most important difference of the finite cell method to the standard finite element approach is the integration over the finite elements (finite cells), which are cut by the boundary (Figure 6). For a more detailed insight into the FCM we refer the reader to the comprehensive review article [9], in which several methods to include Dirichlet and Neumann types of boundary conditions are also presented.

3.2 Integration of the FCM into a commercial FE package

The applied FCM software is a *Matlab* based in-house code that goes back to [17]. It is obvious, that a robust implementation of the FCM methodology within a more widespread and established commercial FEM software tool would create a higher applicability to practical engineering problems. Consequently, a software concept has been developed to couple the FCM with the commercial FEM software package *Abaqus*, where some open-source software products for the pre- and post-processing tasks have been additionally applied. The general workflow of the software concept is illustrated in Figure 7.
It is assumed that all applied pores received from CT investigations are available in a repaired form and ready for FEM simulations. These data are provided in the Step II of the flowchart of Figure 5. For repairing the STL data of the pores the *Simcenter* software is used, but, also any other qualified software tool can also be applied in advance. This is discussed in detail in the following Chapter 3. For the coupling, only freely available software interfaces of *Abaqus* were used [18]. To this end, a user subroutine with help of the *Abaqus* routine UEL has been developed, which is able to incorporate the required functionality. In 3D, the FCM can be applied if the FEM basis elements are hexahedral or tetrahedral finite elements with linear as well as quadratic type

of shape functions. Besides the microstructural data from CT measurements, virtually generated STL data can be applied as well. The initial model is set up in the pre-processing module of *Abaqus*. Here, the material properties and the element types are defined. In the next step an *Abaqus* input file is generated. This file is further processed in *Matlab* and adjusted to incorporate the user defined element routine UEL. At this stage the micro-structural details from CT measurements are added to the analysis and also the necessary details to perform the numerical integration are generated. During the solution of the governing equations these data are read in by the UEL. For post-processing, a geometry-conforming visualization mesh is created. This can be achieved using any powerful external mesh generator. We have used the freely available software *Netgen* [19]. The analysis results are then interpolated onto new visualization nodes using the finite element shape functions of the coupled FEM-FCM model and the results are saved in a *vtk*-file format. This format is further processed by the open source *ParaView* software, which offers all the capabilities of commercial FEM post-processing tools.

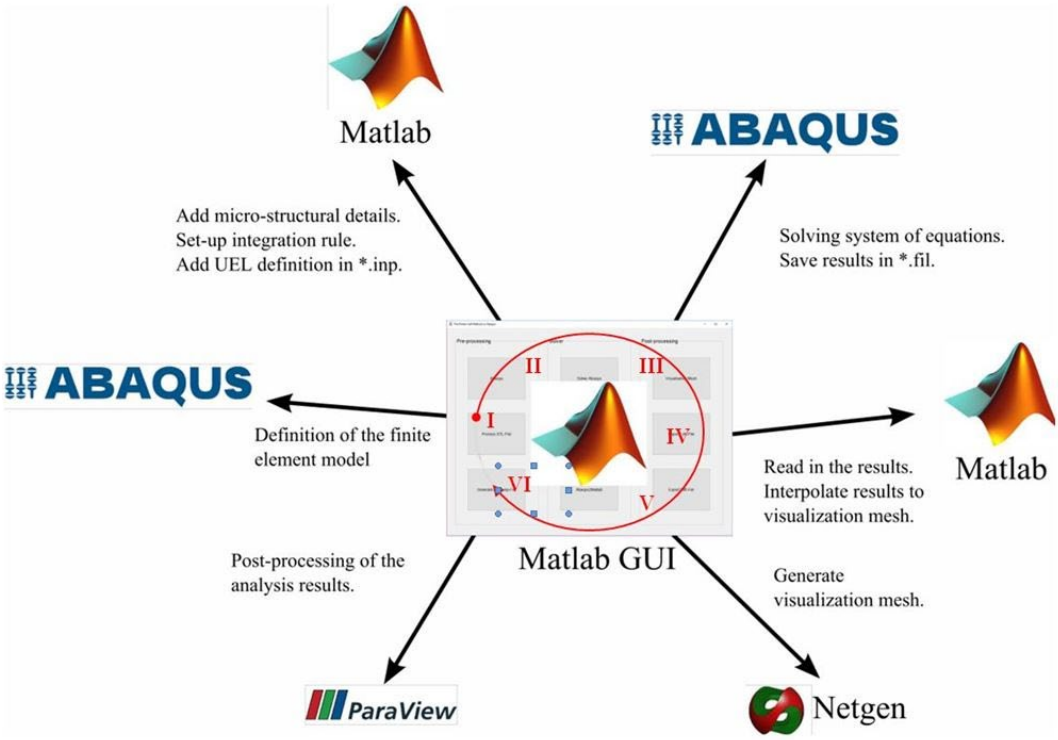

Figure 7. Workflow of coupling the FCM with *Abaqus*; the numbers I-VI denote the sequence of the application of the subprograms; the pores in form of repaired STL data are included in Step II

The developed coupled FEM-FCM concept based on *Abaqus* has been tested with help of several simple test examples and sufficient accurate results were received [20].

4. Industrial Example

The developed procedure is applied at a gearbox housing of a coaxial electric drive system (Figure 8). The housing of the gearbox is manufactured via an aluminum die-casting

process. The input torque of the electric motor is transmitted by a planetary gear. The torque of the ring gear is supported by teeth in the housing. The rotating planets and the elastic deformation of the ring gear cause cyclic stresses in the teeth of the housing, which are the main factors determining the service life of the component. A CT analysis was carried out for the housing of the gearbox and three pores were selected for a systematic investigation (Figure 8).

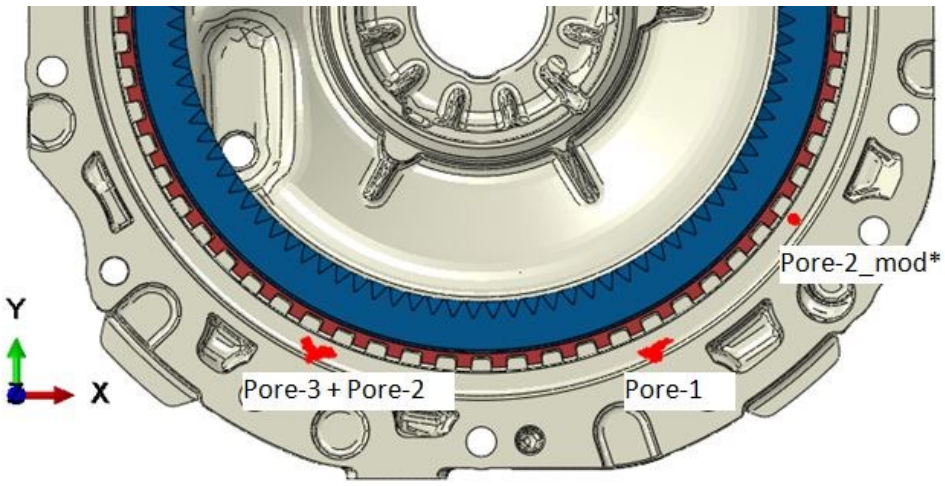

Figure 8. Three pore variants marked in red from CT measurements of the gear housing

In Figure 8, Pore-2 and Pore-3 are located close together while Pore-1 is a large pore and Pore-2_mod is the same as Pore-2 but it has been shifted and rotated to a position close to the root of a gear tooth. For comparison purposes in the following only the stress distribution in the vicinity of the pore-2_mod is shown. The coupled FEM-FCM solution is compared with the results of a pure FEM solution. Both calculations were performed with nearly the same mesh density; the pore has been meshed with an edge length of 0.4 mm in both cases. The maximum stresses (marked in red, see Figure 9) are larger in the pure

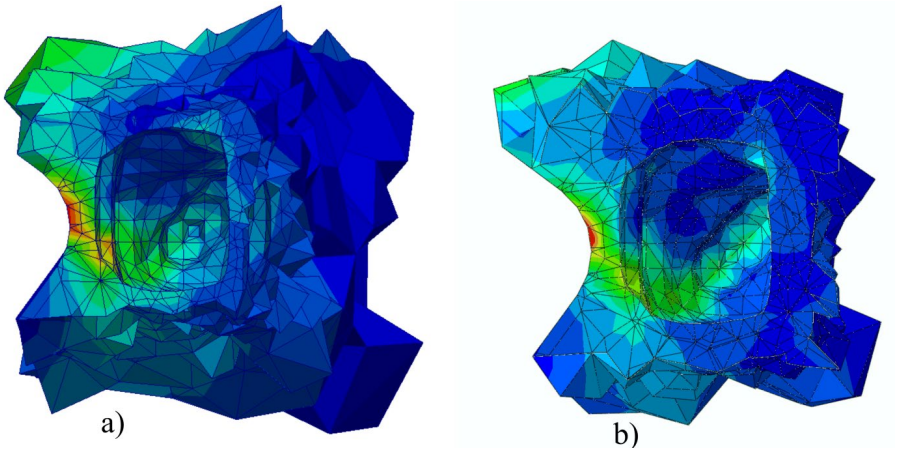

Figure 9 von Mises stresses in the vicinity of pore-2_mod at the root of the tooth.
a) Coupled FEM-FCM solution ($\sigma_{max} = 108\ N/mm^2$). b) Pure FEM solution ($\sigma_{max} = 130\ N/mm^2$)

FEM solution resulting in 130 N/mm^2 in comparison to the coupled FEM-FCM solution of 108 N/mm^2. The reason for this is that in the cut elements of the FCM, a jump in the displacements is smoothed by the shape functions resulting in reduced maximum stresses. This affects the results at the base of the teeth most strongly due to the fact that the cut elements are located directly next to the root of the teeth. This could be overcome by a more refined basis mesh in FEM-FCM approach. For the evaluation of the stresses in the area of the pores themselves, two discretization levels were used in order to be able to assess the influence of the discretization.

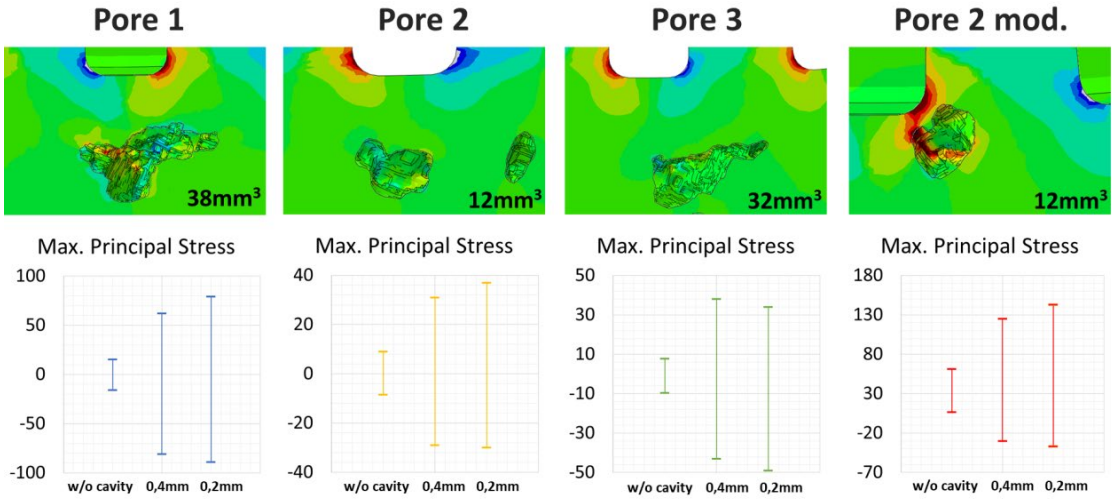

Figure 10. Relative deviations of tooth root stresses without porosity (w/o) in comparison to with porosity calculated with two different pore mesh sizes of 0.4mm and 0.2mm.

It can be seen that the stress increases are in the range of 2 to 5 times that of the local stress of the reference model without pores. For the manually positioned Pore-2_mod, it can be seen that the local stress at the pore is higher than the local stress at the surface of the gear tooth root. Consequently, this would be the dominant stresses for fatigue analysis if periodical load conditions are taken into account. The analysis has shown that large pores will increase the surface stresses, and, consequently, influencing the fatigue behavior and the life span of a part. In our example, it is also shown that a pore with smaller volume but also smaller edge distance is more critical than a pore with a large volume and simultaneously larger edge distance.

5. Summary and Conclusions

The paper shows the importance of taking into account the porosity of aluminium die-cast parts in stress simulations. Pores are unavoidable defects, which significantly influence the fatigue and fracture behaviour of constructions, especially if the structures are subjected to high static, dynamic and cycling loads. The pore data can be obtained from CT measurements or can also be artificially generated in order to investigate their influence on the fatigue behaviour of porous die-cast parts. The quality of the measured pore

geometry depends on the applied voxel size of the CT device. The voxel data and the Hounsfield scale of each voxel are the basis to generate automatically a triangular surface mesh of each pore in form of a STL data set. For further applications of the STL data, such as FEM simulations, it is important that the STL data of each pore are unique and provide a closed surface. This is typically not the case after a CT inspection. Consequently, the STL data have to be repaired to be applicable for further FEM simulations. A very powerful technique is the surface-wrapping, which results in a new convex outer boundary surface of a pore. Al these possibilities are provided by the *Simcenter* software, which is recommended for repairing STL data of pores for a subsequent use of the data. In the paper it is shown that the pores can be taken into account with help of the finite cell method (FCM). The FCM don´t require a body fitted mesh, which is seen as the main advantage of this approach. But, the application of an overall FCM approach of a whole structure is not reasonable, because there are already FEM models available and were applied to design each casted part, without pores. From an application point of view, it would be excellent, if the pores in form of STL data sets could be automatically included in the FEM simulation. In the paper it is shown, how the FCM can be included in the commercially available FEM software package *Abaqus.* The coupled approach has been successfully applied to real engineering problems. The presented example is a gear box housing of an electric drive motor manufactured as an aluminium die-cast part. The coupled FEM-FCM approach is used to investigate different types and distributions of pores, which have been detected by CT inspections and available as SLT data. Alternatively, a pure FEM approach is presented as well, which is also able to take into account pores as STL data. The comparison of the results received with the coupled FEM-FCM approach and the pure FEM analysis has shown that an adequate mesh density of the basis mesh is required, especially in regions with critical stress levels and small pores sizes. The element size of the basis mesh in the surrounding of a pore should be significantly smaller than the dimensions of the pore, even if second order finite elements are used. The simulation results confirm the results of other researchers that a pore with a small edge distance is more critical than a larger pore, but, simultaneously at a greater distance from the edge [21]. The presented approach is helpful in industry to virtually investigate the influence of die-cast pores to the quality of the produced structural parts. This provides a better basis for the decision, whether a produced part is rejecting or not.

References

[1] Campbell, J.: *Complete casting handbook,* Elsevier Ltd. 2011

[2] Zyska, A., Konopka, Z., Łągiewka, M. and Nadolski, M.: Porosity of castings produced by the vacuum assisted pressure die casting method, *Arch. Foundry Eng.,* Vol. 15 (2015), pp. 125–130, doi:10.1515/afe-2015-0023, https://doi.org/10.1515/afe-2015-0023 .

[3] Ambos, W. Besser, S. Teuber, O. Brunke, D. Neuber, Stuke, I. and Lux, H.: Modern methods for determining the porosity in die cast components using fast computer tomography, *International Foundry Research,* Vol. 65, 2013, No. 2, pp. 16-25.

[4] Zhang, Y., Bajaj, C. and Sohn, B.S.: 3D Finite Element Meshing from Imaging Data, *Applied Mechanics and Engineering*, Vol. 179, 1999, pp. 31–52, https://doi.org/10.1016/j.cma.2004.11.026.

[5] Bechet, E., Cuilliere, J. C. and Trochu, F. Generation of a finite element mesh from stereolithography (STL) files, *Computer-Aided Design*, Vol. 34, 2002, pp. 1–17. https://doi.org/10.1016/S0010-4485(00)00146-9

[6] Liu, F., Zhou, H. and Li, D.: Repair of STL errors, *International Journal of Production Research*, 47:1, 2009, pp. 105-118, https://doi.org/10.1080/00207540701424539 .

[7] Attene, M. Direct repair of self-intersecting meshes, *Graphical Models*, Vol. 76, 2014, pp. 658–668, https://doi.org/10.1016/j.gmod.2014.09.002.

[8] Düster, A., Parvizian, J., Yang, Z. and Rank, E.: The finite cell method for three-dimensional problems of solid mechanics, *Computational Methods in Applied Mechanics and Engineering*, Vol. 197, 2008, pp. 3768–3782, https://doi.org/10.1016/j.cma.2008.02.036.

[9] Schillinger, D. and Ruess, M.: The finite cell method: A review in the context of higher-order structural analysis of CAD and image-based geometric models, *Arch. Comp. Meth. Engin*. 22(3), 2015, pp. 391–455, https://link.springer.com/article/10.1007/s11831-014-9115-y.

[10] Duczek, S., Berger, H. and Gabbert, U.: The finite pore method: A new approach to evaluate gas pores in cast parts by combining computed tomography and the finite cell method, *International Journal of Cast Metals Research*, Vol. 28 (2015), 4, pp. 221-228, https://doi.org/10.1179/1743133615Y.0000000003.

[11] Leordean, D., Vilău, C. and Dudescu, M.C.: Generation of computational 3D models of human bones based on STL data and CAD software packages, *Applied Sciences*, 11(17):7964, 2021, https://doi.org/10.3390/app11177964.

[12] Sokac, M., Budak, I., Katic, M., Jakovljevoc, Z., Santosi, Z. and Vukelic, D.: Improved surface extraction of multi-material components for single-source industrial X-ray computed tomography, *Measurements*, Vol. 153, 2020, https://doi.org/10.1016/j.measurement.2019.107438.

[13] Ji, S., Watson, D. and Fan, Z.: X-Ray Computed tomographic investigation of high pressure die castings, in: Ratvik, A. (Ed.): *Light Metals, The Minerals, Metals & Materials Series*, Springer, 2017, https://doi.org/10.1007/978-3-319-51541-0_104.

[14] Anderl, R., Binde, P.: *Simulations with NX / Simcenter 3D*, Carl Hanser Munich 2018, ISBN (Book): 978-1-56990-712-2.

[15] Wang, Q. and Jones, P.E.: Fatigue life prediction in aluminium shape castings, *International Journal of Metalcasting*, Vol. 8, 2014, 3, pp. 29-38, https://doi.org/10.1007/BF03355588.

[16] Duczek, S. and Gabbert, U.: Efficient integration method for fictitious domain approaches, *Computational Mechanics*, Vol. 56, 2015, pp. 725-738, https://link.springer.com/article/10.1007/s00466-015-1197-3 .

[17] Duczek, S.: *Higher order finite elements and fictitious domain concept for wave propagation analysis*, PhD thesis, University of Magdeburg, in Fortschritt-Berichte, 20, No. 437, 2014, Düsseldorf, VDI Verlag 2014.

[18] Würkner, M., Duczek, S., Berger, H., Köppe, H. and Gabbert, U. A software platform for the analysis of porous die-cast parts using the finite cell method, in Altenbach, H., Carrera, E. and Kulikov, G. (Eds.*: Analysis and Modelling of Advanced Structures and Smart Systems, Series: Advanced Structured Materials,* Springer, 2018, pp. 327-341, IBSN: 978-981-10-6764-8.

[19] Schöberl, J.: NETGEN: An advancing front 2D/3D-mesh generator based on abstract rules, *Computing and Visualization in Science*, Vol. 1 (1997), pp. 41–52.

[20] Gabbert, U. and Würkner, M.: Simulation of cellular structures with a coupled FEM-FCM approach based on CT data, *Journal of Computational and Applied Mechanics*, Vol. 16, 2021, No. 1, pp. 57–70, https://doi.org/10.32973/jcam.2021.004.

[21] Le, V.-D., Saintier, N., Morel, F., Bellett, D. and Osmond, P.: Investigation of the effect of porosity on the high cycle fatigue behaviour of cast Al-Si alloy by X-ray micro-tomography, *International Journal of Fatigue*, Volume 196, 2018, pp. 24-37, https://doi.org/10.1016/j.ijfatigue.2017.09.012.